Cooperative Distributed Demand Management for Community Charging of PHEV/PEVs Based on KKT Conditions and Consensus Networks

Navid Rahbari-Asr, *Student Member*, *IEEE*, and Mo-Yuen Chow, *Fellow*, *IEEE*

***Abstract*—Efficient and reliable demand side management techniques for community charging of plug-in hybrid electrical vehicles (PHEVs) and plug-in electrical vehicles (PEVs) are needed, as large numbers of these vehicles are being introduced to the power grid. To avoid overloads and maximize customer preferences in terms of time and cost of charging, a constrained nonlinear optimization problem can be formulated. In this paper, we have developed a novel cooperative distributed algorithm for charging control of PHEVs/PEVs that solves the constrained nonlinear optimization problem using Karush–Kuhn–Tucker (KKT) conditions and consensus networks in a distributed fashion. In our design, the global optimal power allocation under all local and global constraints is reached through peer-to-peer coordination of charging stations. Therefore, the need for a central control unit is eliminated. In this way, single-node congestion is avoided when the size of the problem is increased and the system gains robustness against single-link/node failures. Furthermore, via Monte Carlo simulations, we have demonstrated that the proposed distributed method is scalable with the number of charging points and returns solutions, which are comparable to centralized optimization algorithms with a maximum of 2% sub-optimality. Thus, the main advantages of our approach are eliminating the need for a central energy management/coordination unit, gaining robustness against single-link/node failures, and being scalable in terms of single-node computations.**

***Index Terms*—Consensus algorithms, decentralized control, demand side management, Karush–Kuhn–Tucker (KKT) conditions, plug-in electric vehicle (PEV), plug-in hybrid electric vehicle (PHEV).**

NOMENCLATURE

$w_i(k)$	The priority weighting for the ith vehicle at the kth time step.
$\mathrm{SoC}_i(k)$	State-of-charge (SoC) of the battery of the ith vehicle at the kth time step.
$P_i(k)$	Allocated power to the ith vehicle at the kth time step.
$P_{i,\max}(k)$	The power bound for the ith vehicle at the kth time step.
$P_i(k)^*$	The optimal allocation of power to the ith vehicle at the kth time step.
P_{total}	Maximum total available power for charging.
C_i	The equivalent capacitance of the ith battery.
$V(\mathrm{SoC}_{i,\max})$	Voltage of the battery at maximum charged state.
$V(\mathrm{SoC}_{i,\min})$	Voltage of the battery at minimum charged state.
Q_i	The capacity of the ith battery.
Δt	Time step for charging.
η_i	Efficiency of the charging of the ith battery.
$\mathrm{SoC}_{i,\max}$	The maximum desired SoC.
$\mathrm{SoC}_{i,0}$	The initial SoC of the vehicle, when it connects to the grid.
$\alpha_i(k)$	$w_i(k)\frac{C_i}{Q_i}\sqrt{\frac{2\eta_i\Delta t}{C_i}}$.
$\beta_i(k)$	$\frac{C_i V_i(k)^2}{2\eta_i\Delta t}$.
J_i	Cost function of the ith vehicle.
$\tilde{J}_i$	Approximated cost function of the ith vehicle.
K_{1i}, K_{2i}	Approximation coefficients.
$\alpha_i'(k)$	$K_i(k)\alpha_i(k)$.
N_i	Number of neighbors of agent i.
μ_i	Lagrange multiplier for the local upper bound constraint.
λ	Lagrange multiplier for the global inequality constraint.
U	The set of indices of vehicles that have been allocated with the local upper bound of power.
$z_i(t)$	Consensus variable for $\sum_{j=1,j\notin U}^{N}\alpha_i'(k)^2$.
$q_i(t)$	Consensus variable for $P_{\text{total}}-\sum_{i\in U}\tilde{P}_{i,\max}$.

Manuscript received June 18, 2013; revised November 11, 2013; accepted January 22, 2014. Date of publication February 03, 2014; date of current version August 05, 2014. This work was supported in part by the National Science Foundation (NSF) under Award EEC-0812121. Paper no. TII-13-0398.

The authors are with the Department of Electrical and Computer Engineering, North Carolina State University, Raleigh, NC 27606 USA (e-mail: nrahabr@ncsu.edu; chow@ncsu.edu).

Color versions of one or more of the figures in this paper are available online at http://ieeexplore.ieee.org.

Digital Object Identifier 10.1109/TII.2014.2304412

I. INTRODUCTION

TECHNOLOGIES used to update utility electricity systems with computer-based automation and control through two-way communications structures constitute the core of the "smart grid" concept [1]. Enabling the transition to plug-in hybrid electrical vehicles (PHEVs) and plug-in electrical vehicles (PEVs) is one of the anticipated benefits of the smart grid [2]. These vehicles provide many incentives for the transportation industry and the environment [3]. Large-scale integration of these vehicles has potential impacts and benefits for the grid. One of the apparent impacts is the increase of the peak demand [4], which can destabilize the grid if not managed properly. On the other hand, the PHEV/PEVs can benefit the grid by being treated as a flexible load through charge/discharge scheduling to shape the load profile [4], [5]. Moreover, on the customer side, the increased satisfaction from the charging process in terms of

time and cost of charging as well as the state-of-charge (SoC) of the vehicle, when leaving the charging station, can improve the adoption rate of the electric vehicles (EVs). Therefore, employing efficient energy-management policies to control and optimize the charging process for EVs is becoming a critical need for the future grid. The enabling technology is called vehicle-to-grid (V2G) technology [6]. In general, V2G technology is operated in a large scale and involves optimization strategies with single or multiple objectives [7]. The process of optimal dispatch of PHEV/PEVs using the V2G technology is called "smart charging" [8], [9]. The focus of this paper is on a "smart charging" method using unidirectional V2G technology.

The existing smart-charging approaches for PHEV/PEV charging in the literature, in most cases, are centralized. The charging stations are required to transmit data to a control center called aggregator [7]. The control center performs the necessary computations and determines the optimal power allocation for each unit and transmits it to the charging stations [10]–[13]. The centralized approach works well for small-scale problems with a small number of vehicles where each unit can send information to the central controller directly without congestion. However, as the number of PHEVs/PEVs increases and they spread over a wide zone, such as a large city, the centralized approach loses efficiency due to two main reasons.

1) The required communications and computational capacity of the control center grows as the dimension of the problem increases.
2) The system becomes fragile to single points of failure.

To solve the issues of centralized smart charging for large-scale problems, research has started on decentralized PHEV/PEV demand control. In most of the proposed decentralized approaches in the literature, each charging station regulates its own power by responding to an external signal [14]–[19]. Therefore, the computational burden is relieved from the control center. However, still a center/aggregator is required to send the coordinating/pricing signals. Specifically, in [14], low-voltage transformers coordinate with each other by communicating with a high-voltage transformer to reduce the imbalances; in [15]–[17], the utility sends a central price/event signal to all the charging stations to manage the aggregate charging load; in [18], the distributed units respond to changes in the price signal adjusted through a center; and in [19], a hierarchical decentralized method is introduced in which central aggregator broadcasts update/average information back and forth to/from sub-aggregators and in some cases, the global constraint to avoid overloads is violated.

In this paper, we introduce a cooperative distributed optimal power-allocation algorithm to satisfy grid constraints and customer preferences for large-scale charging of PHEVs/PEVs. Unlike the aforementioned decentralized approaches, our algorithm is completely center-free. It works based only on the local sharing of information among the charging stations and has no central aggregator/coordinator unit. Consequently, single-node congestion is alleviated, and the system becomes more robust against single points of failures. Moreover, the computational and communications burden is divided among the distributed processors, so the proposed approach is scalable. Unlike approaches that are based on dual decomposition (e.g., [19]), in our algorithm prior to the convergence, the global constraint is never violated.

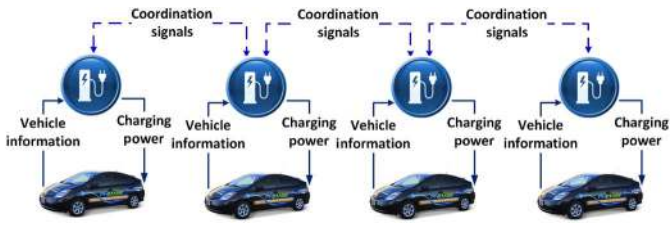

Fig. 1. Cooperatives distributed demand management for PHEV/PEV community charging.

The idea of our algorithm is shown in Fig. 1. Related work is done in [20]. The current paper explains the algorithm in theoretical details and studies its scalability and sub-optimality and compares it with centralized algorithms. Similar concepts are also used in our research group to optimally manage distributed energy resources on the generation side [21].

Organization of this paper is as follows. Section II provides the problem statement. In Section III, we propose our distributed consensus-based algorithm. Section IV presents the numerical analysis and results, and the concluding remarks are made in Section V.

II. Problem Formulation for Large-Scale Optimization of PHEV/PEV Charging

The problem of PHEV/PEV community charge allocation can be formulated as an optimization problem consisting of an objective function and appropriate constraints.

A. Objective Function

Different factors, such as battery longevity [10], the amount of charge and tightness of the deadline [11], flattening of the overall load profile and reduction of the load variance [22], and the cost of charging for vehicle owners [17], can be considered in defining the objective function for PHEV/PEV charge coordination.

Satisfaction of the PHEV/PEV users from the charging service is directly related to the SoC of the vehicle, when leaving the charging station. Therefore, in this paper, similar to [12], the objective function is defined as the weighted sum of the SoC of the vehicles at the next time step

$$\underset{\boldsymbol{P}(k)}{\text{Max}}\ J = \sum_{i=1}^{N} w_i(k)\text{SoC}_i(k+1) \tag{1}$$

where $\boldsymbol{P}(k) = [P_i(k)]_{i=1,\ldots,N}$ is the vector of the power allocated to the vehicles, N is the total number of vehicles, $\text{SoC}_i(k+1)$ is the SoC of the battery pack of the ith vehicle at the next iteration, and $w_i(k)$ is the priority weighting for the ith vehicle, as well as a non-negative value. Depending on the desired performance, the weights can prioritize vehicles based on the remaining time of charge, remaining battery capacity to be charged, and/or the customer's willingness to pay.

B. Relationship Between SoC and Charging Power

The objective function is defined in terms of the SoC because, on the customer side, the SoC of the vehicle at the end of the

charging period is the main issue of concern. To find the relationship between the allocated power for charging and the SoC, we need a model for the battery. In a certain operating range, the battery can be modeled as a capacitor circuit. In this range, the variation of the SoC is proportional to the variation of the battery voltage. More complicated battery models can be considered in the optimization process, and this would be one of the future works of the authors. Considering the capacitance model, the equivalent capacitance of the ith battery C_i is then calculated as

$$C_i = \frac{Q_i\left(\mathrm{SoC}_{i,\max} - \mathrm{SoC}_{i,\min}\right)}{V(\mathrm{SoC}_{i,\max}) - V(\mathrm{SoC}_{i,\min})} \tag{2}$$

where Q_i is the capacity of the ith battery in Coulombs and $[\mathrm{SoC}_{i,\min}, \mathrm{SoC}_{i,\max}]$ is the operating range of the battery. The change in the charge of the battery at each time step k would be $\Delta q_i = \Delta C_i V_i(k)$. So, we can write

$$\mathrm{SoC}_i(k+1) - \mathrm{SoC}_i(k) = \frac{C_i V_i(k+1) - C_i V_i(k)}{Q_i}. \tag{3}$$

The energy provided to the battery during each time step Δt would be $P_i \Delta t$. Considering the efficiency of the charging to be η_i, the energy stored in the battery would equal $\eta_i P_i \Delta t$. Applying conservation of energy

$$\frac{1}{2} C_i V_i(k+1)^2 - \frac{1}{2} C_i V_i(k)^2 = \eta_i P_i \Delta t. \tag{4}$$

Substituting for $V_i(k+1)$ from (4) into (3) yields

$$\mathrm{SoC}_i(k+1) = \mathrm{SoC}_i(k) + \frac{C_i}{Q_i}\left(-V_i(k) + \sqrt{V_i(k)^2 + \frac{2\eta_i P_i(k)\Delta t}{C_i}}\right). \tag{5}$$

C. Constraints

Constraints represent the physical limits.

1) Global Constraint: There is a limit on the total amount of power that the utility can allocate for charging purposes P_{total}. It is modeled as the upper bound of the utility's power delivery

$$\sum_{i=1}^{N} P_i(k) \le P_{\mathrm{total}}. \tag{6}$$

2) Local Constraint: Certain factors impose local bounds on the amount of allocated power for each unit; for instance, the maximum power output of the outlet (e.g., 4.6 kW for a standard single-phase 230-V outlet), level of charging (e.g., 1.33 kW for level 1), the maximum tolerable charging current $I_{\max}$, and the maximum allowable SoC ($\mathrm{SoC}_{\max}$) to avoid overcharging. These constraints are mapped into one constraint for each unit

$$0 \le P_i(k) \le P_{i,\max}(k) \quad \forall i = 1, \ldots, N \tag{7}$$

where $P_{i,\max}(k)$ is the upper bound of the allocated power considering all the local limitations. As the V2G capability is not considered here, the lower bound is set to zero, so the PHEV/PEVs should not be discharged.

D. Optimization Problem Structure

Substituting for $\mathrm{SoC}_i(k+1)$ from (5) into (1)

$$\underset{P(k)}{\mathrm{Max}}\ J = \sum_{i=1}^{N} w_i(k)\mathrm{SoC}_i(k) - \sum_{i=1}^{N} \frac{C_i}{Q_i} V_i(k) + \sum_{i=1}^{N} w_i(k)\sqrt{V_i(k)^2 + \frac{2\eta_i P_i(k)\Delta t}{C_i}}. \tag{8}$$

The first two summations in (8) are independent of the decision variables $P_i(k)$ and, therefore, can be eliminated from the objective function

$$\underset{\boldsymbol{P}(k)}{\mathrm{Max}}\ J = \sum_{i=1}^{N} w_i(k)\sqrt{V_i(k)^2 + \frac{2\eta_i P_i(k)\Delta t}{C_i}}. \tag{9}$$

To simplify the notations, we introduce $\alpha_i(k) = w_i(k)\frac{C_i}{Q_i}\sqrt{\frac{2\eta_i \Delta t}{C_i}}$ and $\beta_i(k) = \frac{C_i V_i(k)^2}{2\eta_i \Delta t}$ and rephrase (9) as

$$\underset{\boldsymbol{P}(k)}{\mathrm{Max}}\ J = \sum_{i=1}^{N} \alpha_i(k)\sqrt{P_i(k) + \beta_i(k)}. \tag{10}$$

Considering the constraints, the optimization problem in terms of the allocated charging powers can be expressed as

$$\underset{\boldsymbol{P}(k)}{\mathrm{Min}}\ J = -\sum_{i=1}^{N} \alpha_i(k) J_i(k) = -\sum_{i=1}^{N} \alpha_i(k)\sqrt{P_i(k) + \beta_i(k)}$$

$$\text{subject to:}$$

$$\sum_{i=1}^{N} P_i(k) \le P_{\mathrm{total}}$$

$$0 \le P_i(k) \le P_{i,\max}(k) \quad \forall i = 1, \ldots, N. \tag{11}$$

Remark 1: More charging power for each unit results in a higher SoC for the vehicle and therefore higher satisfaction for the customers. That is why the objective function in (11) is a monotonically increasing function in terms of the charging power. If there was no limit on the total available charging power, the optimal allocation of power for all the vehicles would be the upper limit of the charging power at each charging station. However, as the total available power is limited by the grid constraints, the optimal allocation of power for each unit would not necessarily be equal to the boundary value.

III. Distributed Charging Algorithm

Our distributed charging algorithm is based on Karush–Kuhn–Tucker (KKT) conditions of optimality [23].

A. KKT Conditions of Optimality

Consider the general optimization problem of the form

$$\begin{aligned} &\text{Min } J(x) \text{ subject to:} \\ &h_i(x) = 0 \quad \forall i = 1, \ldots, n \\ &g_j(x) \leq 0 \quad \forall j = 1, \ldots, m. \end{aligned} \tag{12}$$

If x^* is a solution of (12), then there are constants $\lambda_i (i = 1, \ldots, n)$ and $\mu_i (i = 1, \ldots, m)$, called KKT multipliers [23], such that

$$\nabla J(x^*) + \sum_{i=1}^{n} \lambda_i \nabla h_i(x^*) + \sum_{i=1}^{m} \mu_i \nabla g_i(x^*) = 0 \tag{13}$$

$$h_i(x^*) = 0 \quad \forall i = 1, \ldots, n$$

$$g_i(x^*) \leq 0 \quad \forall i = 1, \ldots, m \tag{14}$$

$$\mu_i g_i(x^*) = 0 \quad \forall i = 1, \ldots, m \tag{15}$$

$$\mu_i \geq 0 \quad \forall i = 1, \ldots, m. \tag{16}$$

The conditions (13)–(16) are called KKT conditions and are necessary for optimality. When the objective function is convex and the constraints are affine (as in our case), the KKT conditions are sufficient for global optimality as well [23].

B. Nonlinear Approximation of the Cost Function

In order to simplify the optimization process, we approximate $J_i = \sqrt{P_i(k) + \beta_i(k)}$ in (11) with $\tilde{J}_i = K_{1i}(k)\sqrt{P_i(k)} + K_{2i}(k)$ and choose $K_{1i}(k)$ and $K_{2i}(k)$ to minimize the norm of the difference between J_i and $\tilde{J}_i$ for $0 \leq P_i(k) \leq P_{i,\max}(k)$

$$[\, K_{1i}(k)^* \quad K_{2i}(k)^* \,] = \arg \min_{K_{1i}(k), K_{2i}(k)} \left\| J_i(k) - \tilde{J}_i(k) \right\|_2^2. \tag{17}$$

By solving (17)

$$\begin{aligned} {K_{1i}}^*(k) = {} & 9{P_{i,\max}}^{-1}\sqrt{{P_{i,\max}}^2 + \beta P_{i,\max}} \\ & - 8{P_{i,\max}}^{-3/2}\left(\beta + P_{i,\max}\right)^{3/2} \\ & + 8\beta^{3/2}{P_{i,\max}}^{-3/2} - 2.5\beta^2{P_{i,\max}}^{-2} \\ & \times \ln\left(\beta/2 + P_{i,\max} + \sqrt{P_{i,\max}\left(\beta + P_{i,\max}\right)}\right) \\ & + 4.5\beta{P_{i,\max}}^{-2}\sqrt{{P_{i,\max}}^2 + \beta P_{i,\max}} \\ & + 2.5\beta^2{P_{i,\max}}^{-2}\ln(\beta/2) \\ {K_{2i}}^*(k) = {} & -3\left(2{P_{i,\max}}^{-1/2}\sqrt{{P_{i,\max}}^2 + \beta P_{i,\max}}\right) \\ & + 2{P_{i,\max}}^{-1}\left(\beta + P_{i,\max}\right)^{3/2} \\ & + 2\beta^{3/2}{P_{i,\max}}^{-1} - 0.5\beta^2{P_{i,\max}}^{-3/2} \\ & \times \ln\left(\beta/2 + P_{i,\max} + \sqrt{P_{i,\max}\left(\beta + P_{i,\max}\right)}\right) \\ & + \beta{P_{i,\max}}^{-3/2}\sqrt{{P_{i,\max}}^2 + \beta P_{i,\max}} \\ & + 0.5\beta^2{P_{i,\max}}^{-3/2}\ln(\beta/2). \end{aligned} \tag{18}$$

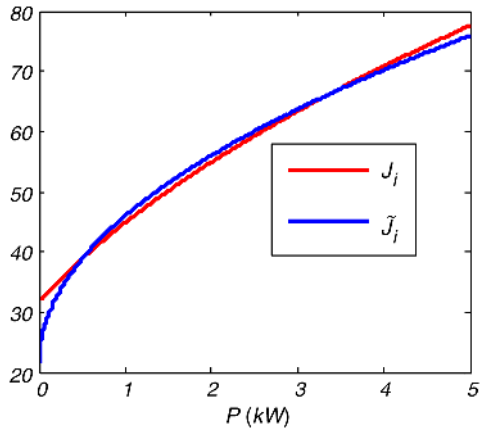

Fig. 2. Actual objective function and the approximated objective function.

With this approximation, we can write the optimization problem as (19) where $\alpha_i'(k) = K_{1i}^*(k)\alpha_i(k)$. Note that as $K_{2i}^*(k)$ is a constant addition, it can be eliminated from the objective function

$$\begin{aligned} &\underset{\boldsymbol{P}(k)}{\text{Min}}\ J = -\sum_{i=1}^{N} \alpha_i'(k)\sqrt{P_i(k)} \\ &\text{subject to:} \\ &\sum_{i=1}^{N} P_i(k) \leq P_{\text{total}},\ 0 \leq P_i(k) \leq P_{i,\max}(k)\ \forall i = 1, \ldots, N. \end{aligned} \tag{19}$$

Fig. 2 shows the curves of $J_i(k)$ and $\tilde{J}_i(k)$ for $\beta = 1000$, and $P_{i,\max}(k) = 5$ kW. The effect of this approximation on the optimality of the solutions is studied in Section IV.

C. Solution to the Optimization Problem

By applying the first KKT condition (13) for the optimization problem defined in (19), we get

$$\frac{-\alpha_i'(k)}{2\sqrt{P_i(k)^*}} + \lambda + \mu_i - \xi_i = 0 \quad \forall i = 1, \ldots, N \tag{20}$$

where λ is the KKT multiplier associated with the global inequality constraint and μ_i and ξ_i for $i = 1, \ldots, N$ are associated with the local constraints (one for each of the bounds). If the local inequality constraints are strictly satisfied at the optimal point, based on (15), we would have $\mu_i = \xi_i = 0$. Applying this to (20), we get a positive value for λ, which indicates that $\sum_{i=1}^{N} P_i(k) = P_{\text{total}}$ based on condition (15). Solving for $P_i(k)^*$

$$P_i(k)^* = \frac{\alpha_i'(k)^2}{\sum_{j=1}^{N} \alpha_j'(k)^2} P_{\text{total}} \quad \forall i = 1, \ldots, N. \tag{21}$$

The value for $P_i(k)^*$ already satisfies the non-negativity constraint. This trait is the direct result of the approximation in Section II-B. In order to guarantee that the upper bound limits are also satisfied, we set those values of $P_i(k)^*$ that violate the local maximum bound to their maximum value and exclude their

values from P_{total}. Then, we use the same procedure in (21) to allocate the remaining power to the remaining vehicles. These iterations are repeated until all vehicles receive a valid allocation of power. This method of allocating powers terminates in a maximum of N iterations, and the final point satisfies the KKT conditions of optimality. Because of space limitations, we skip the proof.

D. Distributed Implementation of the Algorithm

The method explained in Section II-C can be implemented in a distributed fashion. The required global information to assign the powers to the remaining vehicles would be the terms $\sum_{j=1,j\notin U}^{N} \alpha'_j(k)^2$ and $P_{\text{total}} - \sum_{j\in U} \tilde{P}_{j,\max}(k)$, where U is the set of indices of all the vehicles allocated with their maximum allowable power. Each of these terms is composed of the summation of some local information. We introduce two consensus variables $z_i(t)$ and $q_i(t)$ for the ith unit to access the global information using a local sharing of information with neighbors, based on consensus algorithms [24], [25].

Table I shows the step-by-step algorithm for finding the optimal power allocation at the ith node. The first step is initialization. For all $i = 1, \ldots, N$, the z_i variable is initialized as $\alpha'_i(k)^2$ and q_i is initialized as zero, except in one of the nodes where the q variable is initialized as P_{total}. Without the loss of generality, this node is indexed as 1. The second step is the consensus phase. During this phase, each charging station updates its z and q variables according to

$$\begin{aligned} z_i(t+1) &= z_i(t) + \sum_{j\in N_i} w_{ij}\big(z_j(t) - z_i(t)\big) \\ q_i(t+1) &= q_i(t) + \sum_{j\in N_i} w_{ij}\big(q_j(t) - q_i(t)\big) \end{aligned} \tag{22}$$

where N_i is the set of neighbors of node i, and $w_{ij} = w_{ji}$ are connectivity strengths, which are chosen such that $0 \le w_{ij} \le (\max_{i=1\ldots N}|N_i|)^{-1}$. It can be shown that with this choice of connectivity strengths, consensus values converge to the average of the initial values of all the nodes if the nodes form a connected group (i.e., if there is a path via neighbors between any two nodes) [16].

Equation (22) can also be represented in the matrix form as

$$\begin{bmatrix} Z(t+1) \\ Q(t+1) \end{bmatrix} = \boldsymbol{W} \times \begin{bmatrix} Z(t) \\ Q(t) \end{bmatrix} \tag{23}$$

where

$$\begin{aligned} Z(t) &= [\, z_1(t) \quad \cdots \quad z_N(t) \,]^T, \\ Q(t) &= [\, q_1(t) \quad \cdots \quad q_N(t) \,]^T \end{aligned} \tag{24}$$

and

$$\boldsymbol{W}(i,i) = 1 - \sum_{j\in N_i} w_{ij}, \quad \boldsymbol{W}(i,j) = w_{ij}. \tag{25}$$

At steps 3–5, each individual charging station uses the global information from the consensus phase along with its own local information to decide about its power allocation by calculating $P_i(k)^{**}$ as

$$P_i(k)^{**} = \frac{q_i(T)}{z_i(T)}\alpha'_i(k)^2. \tag{26}$$

Equation (26) basically evaluates (21) by noting that consensus values have converged to the average of their initial values

$$\begin{aligned} \frac{q_i(T)}{z_i(T)}\alpha'_i(k)^2 &= \frac{P_{\text{total}}/N}{\sum_{j=1}^{N}\alpha'_j(k)^2/N}\alpha'_i(k)^2 \\ &= \frac{\alpha'_i(k)^2}{\sum_{j=1}^{N}\alpha'_j(k)^2}P_{\text{total}}. \end{aligned} \tag{27}$$

If $P_i(k)^{**}$ exceeds $P_{i,\max}(k)$, the charging station allocates $P_{i,\max}(k)$ as the optimal allocation of power and subtracts $\alpha'_i(k)^2$ from its z variable and $P_{i,\max}(k)$ from its q variable to eliminate the information of charging station i in subsequent consensus phases. The charging stations that have already reached their power limit ($P_{i,\max}(k)$) will not change their power allocation in subsequent iterations of the algorithm. Step 6 of the algorithm closes the loop; the algorithm goes back to step 2 and another consensus phase starts. The distributed algorithm for each node will terminate if no change in the consensus values occurs after the consensus phase. Due to the cooperative distributed nature of this algorithm, we call it the cooperative distributed PHEV/PEV demand management (CDPDM) algorithm.

TABLE I
COOPERATIVE DISTRIBUTED PHEV/PEV DEMAND MANAGEMENT (CDPDM) ALGORITHM

1. **Initialize variables**

$z_i(0) = \alpha'_i(k)^2$, if $i = 1: q_i(0) = P_{\text{total}}$, if $i \neq 1: q_i(0) = 0$, flag $= 0$, $P_i(k)^{**} = 0$

2. **Consensus phase**

$t = 0$;
While $t \le T$
$z_i(t+1) = z_i(t) + \sum_{j\in N_i} w_{ij}\big(z_j(t) - z_i(t)\big)$;
$q_i(t+1) = q_i(t) + \sum_{j\in N_i} w_{ij}\big(q_j(t) - q_i(t)\big)$;
$t = t + 1$;
End

3. **Check if** $\|z_i(T) - z_i(0)\| < \varepsilon_0$: Yes: $P_i(k)^* = P_i(k)^{**} \rightarrow$ Terminate; No: $\rightarrow$ Continue

4. **Check if** flag $= 0$: Yes $\rightarrow P_i(k)^{**} = \frac{q_i(T)}{z_i(T)}\alpha'_i(k)^2$; No $\rightarrow P_i(k)^{**} = P_{i,\max}(k)$

5. **Check if** $(\text{flag} = 0) \wedge \big(P_i(k)^{**} \ge P_{i,\max}(k)\big)$

Yes: flag $= 1$; $P_i(k)^{**} = P_{i,\max}(k)$;
$z_i(0) = z_i(T) - \alpha'_i(k)^2$; $q_i(0) = q_i(T) - \tilde{P}_{i,\max}(k)$;
No: $z_i(0) = z_i(T)$; $q_i(0) = q_i(T)$;

6. **Go back to 2. Consensus phase.**

Remark 2: One of the requirements for the proposed cooperative distributed algorithm is connectivity for the communications network. Considering that the power grid network and the power feeders form a physically connected system, the connectivity for the communications network can be realized by having a communications network similar to the physical power network.

IV. Simulation Results and Analysis

This section presents the performance of the proposed distributed algorithm in Section III under different case studies. In all the case studies, each charging station is running the cooperative distributed algorithm shown in Table I. The algorithm is initialized every Δt s, which is the optimization step. During each optimization step, the algorithm keeps running an inner loop between steps 2 and 6.

In all the case studies, the rationale for choosing the proper parameter values is as follows: battery voltage ranges and capacities are typical values for the PHEV/PEV batteries taken from standard charging profiles such as the ones in [26]. SoC can be any value between 0 and 1, and for the case studies, it is randomly selected for each EV. Arrival/departure times are also random and different PHEVs/PEVs can arrive and depart at different times and the maximum available power for each charging station ($P_{\max}$) is determined by the charging level (e.g., 3.3 kW for single-phase, level 2 charging) and battery constraints.

The first case study shows how the algorithm works during each optimization step, and the second case study considers the successive usage of the algorithm in the long run. The robustness of the algorithm to link/node failures is also tested. To make the demonstrations tractable, the number of charging stations in the first two case studies is kept at five. The communications topology between charging stations is chosen similar to the power network topology as shown in Fig. 3. If a single link/node fails in this topology, the rest of the graph will still remain connected and thus, the remaining nodes would be able to continue cooperation with others, via consensus.

The third experiment studies the scalability of the algorithm. The fourth experiment studies the sub-optimality of the algorithm by benchmarking it against conventional centralized optimization methods. For these experiments, Monte Carlo simulations are used.

A. Case Study 1: Single-Step Optimization

A parking deck with five charging stations is considered. The objective is to optimally allocate the available power based on the priority of the vehicles. The priority for the ith vehicle is set as

$$w_i(k) = \frac{1}{\mathrm{SoC}_i(k) TtS_i(k) + \varepsilon} \tag{28}$$

where $TtSi(k)$ is the amount of time, the ith vehicle is going to stay at the charging station, and ε is a positive value introduced to avoid division by zero. Thus, the vehicles with lower SoC and sooner leaving time have higher priority for getting charged. At the kth time step, the information regarding the battery side of the vehicles is given in Table II.

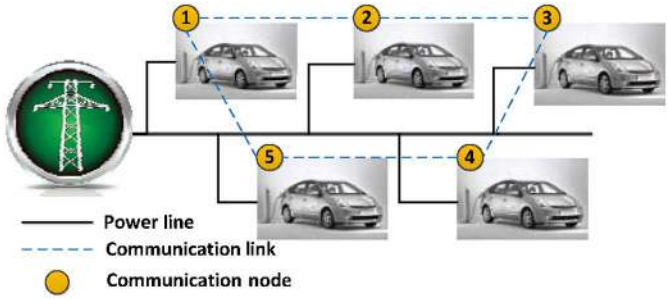

Fig. 3. Communication and power network topologies for case studies 1 and 2.

TABLE II
Information About the Vehicles in the First Case Study

	V_i	$\widetilde{P}_{i,\max}$ (kW)	SoC	TtS (h)	Q (A.h)
Vehicle1	[238–248]	3.3	0.7	6.0	20
Vehicle2	[240–250]	3.3	0.2	3.5	22
Vehicle3	[242–247]	3.3	0.5	2.0	25
Vehicle4	[236–246]	3.3	0.5	8.0	24
Vehicle5	[243–252]	3.3	0.1	1.0	22
Total available power, P_{total}					10 kW
Charging efficiency η					0.9

The maximum number of neighbors of each node is two, so according to the condition $0 \leq w_{ij} < (\max_{i=1,..,N}|N_i|)^{-1}$, any connectivity strength between 0 and 0.5 can be chosen to ensure stability. Using a small value for the connectivity strengths results in a slow convergence of the consensus algorithm. We set all the connectivity strengths equal to 0.4, which is in the feasible range for stability ($0 < 0.4 < 0.5$) and is not small. In general, the optimal selection of the connectivity strengths to achieve fast convergence is itself an optimization problem that has been described in [27] and is outside the scope of this paper. The sampling time for the consensus phase is 1 ms and each consensus phase consists of 50 iterations.

Fig. 4 shows the allocated power and the evolution of the consensus variables over time. At the end of the first consensus phase ($t = 0.05$), the fifth charging station reaches its maximum power boundary. So, it subtracts its local information from its consensus values (z_5 and q_5) according to step 5 of the algorithm. This causes the average of the consensus variables to decrease. Consequently, the consensus variables converge to a new equilibrium point (their new average), which causes other charging stations to receive more power (because charging station 5 cannot consume any more power). Convergence to the new equilibrium is seen as big drops in the plots of the consensus variables.

By the end of the second consensus phase ($t = 0.1$), charging station 2 reaches its maximum bound, which allows other stations to receive more power. By the end of the third consensus phase ($t = 0.15$), all the available power is allocated and all the charging stations have received power in their feasible range. Therefore, the consensus variables do not change any more and the algorithm settles down.

Now, we consider a link failure between nodes 1 and 2 at time $t = 0.01$. Upon link failure, the two nodes can no longer

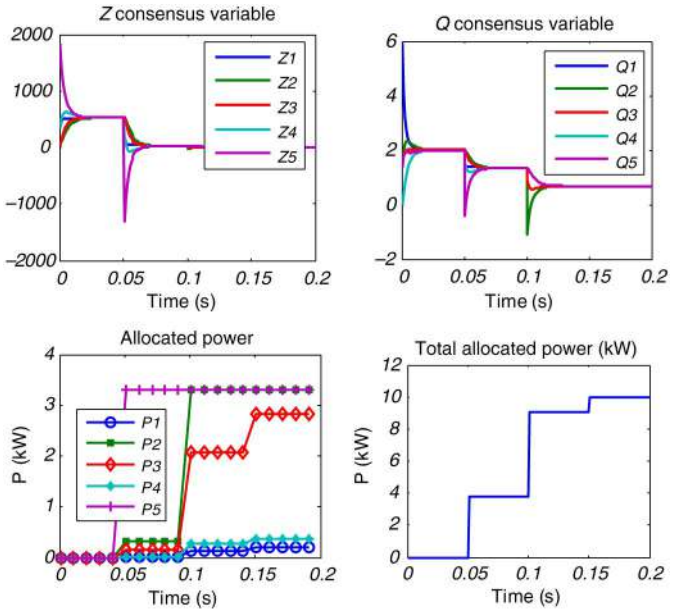

Fig. 4. Allocation of power and evolution of consensus states for case study 1 with no link failure.

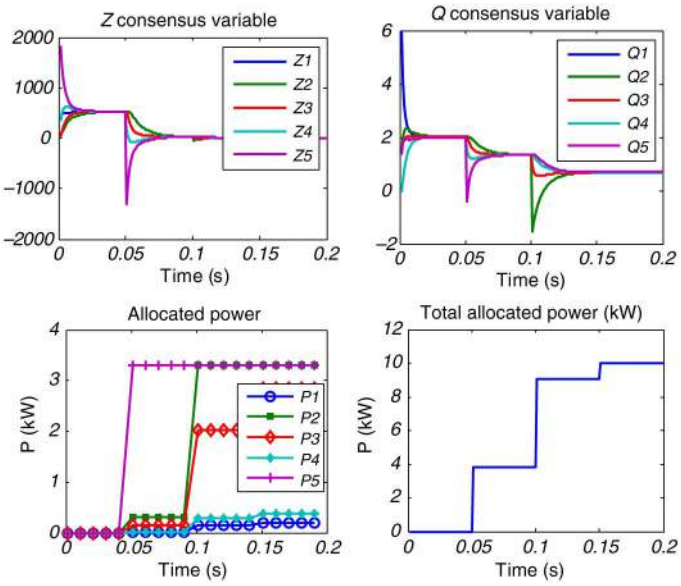

Fig. 5. Allocation of power and evolution of consensus states for case study 1 with single-link failure.

exchange information with each other. When such a failure occurs, the connectivity strength between the two nodes becomes zero, namely $w_{12} = w_{21} = 0$. Fig. 5 shows the allocated power and the evolution of the consensus states. The charging stations can still converge to the same power allocation as shown in Fig. 4. As mentioned in Remark 2, the connectivity of the communications graph is the only requirement of the communications topology in order for the algorithm to work properly. This is the direct result of using consensus algorithms, which can work under switching topologies. After the link failure, the communications network remained connected, and the algorithm was able to converge. However, due to the loss of a connection

TABLE III
INFORMATION ABOUT THE VEHICLES IN THE SECOND CASE STUDY

	SoC_0	$P_{i,max}$ (kW)	I_{max} (A)	Q (A.h)	Arrival (h)	Departure (h)
Vehicle1	0.1	3.3	12	20	0	6
Vehicle2	0.1	3.3	12	22	0	3.5
Vehicle3	0.5	3.3	12	25	1	2
Vehicle4	0.2	3.3	12	24	2	8
Vehicle5	0.3	3.3	12	22	3	6
Total available power, P_{total}					5 kW	
Charging efficiency η					0.9	

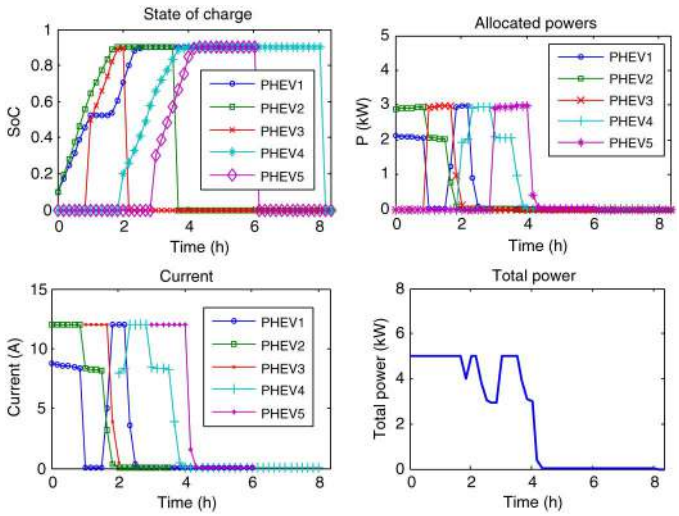

Fig. 6. Charging profiles for case study 2 with no node failure.

link, the convergence during the consensus phases had been slowed down, especially in the second and third consensus phases.

B. Case Study 2: Dynamic Optimization

In this part, we study the behavior of the algorithm in long run. The vehicles arrive and depart at different times. Moreover, for the vehicles inside the charging stations, parameters such as SoC and voltage change due to the charging process. So, the optimization becomes dynamic and the single-step optimization problem to be solved (as in case study 1) keeps changing.

Five vehicles with different initial SoCs and different arrival and departure times are considered as shown in Table III. The desired SoC is 0.9 and the maximum power output of each station is 3.3 kW. The priority weights are defined similar to case study 1. We simulate the distributed charging control model for 8 h. The charging stations change their power allocation every 10 min. Fig. 6 shows the charging profiles of the vehicles over time. At time $t = 0$, two PHEVs are in the charging stations. PHEV2 has an earlier departure time and, therefore, gets higher charging rate. At time $t = 1$ h, PHEV3 arrives at the charging station. As PHEV3 needs to leave very soon, its priority for getting power is higher than those of PHEV1 and PHEV2. At this time, PHEV1, which leaves later than the others, has the lowest priority. Therefore, its charging power drops to near zero, to allow PHEV3 to get more charging power. At time $t = 2$ h,

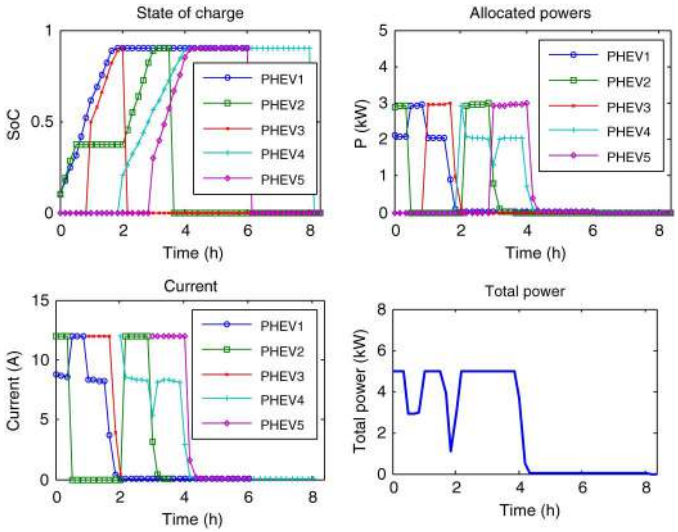

Fig. 7. Charging profiles for case study 2 with node failure.

PHEV3 leaves with $\mathrm{SoC} = 0.9$. The allocation of power during the rest of the time can be explained similarly. We can see that at all times, the total consumed power is below 5 kW. The current profiles are drawn to show that the charging currents resulted from the optimization process are within the feasible boundaries (i.e., $I \leq I_{\max} = 12$ A). This is done by translating the boundary on the charging current into a boundary on the charging power via multiplying it by the terminal voltage of the battery. This boundary then serves as a local constraint for the optimization problem.

Now, we consider the case where node 2 fails to operate at $t = 0.5$ h and recovers at $t = 2$ h. Fig. 7 shows the charging profiles under this scenario. Upon failure, node 2 loses its connection with all its neighbors. However, the rest of the nodes remain connected. When node 2 fails, its charging rate drops down to zero and no change happens in the SoC of the respective vehicle. When node 2 recovers at $t = 3$ h, PHEV2 starts to be charged again. Similar to the case without node failure, all the local and global constraints are satisfied.

Remark 3: To see why the algorithm is robust against single-link/node failures, we note that information exchange is happening through the consensus algorithm

$$z_i(t+1) = z_i(t) + \sum_{j \in N_i} w_{ij}\big(z_j(t) - z_i(t)\big), \quad i = 1, \ldots, N. \tag{29}$$

The global information is the summation of local information

$$\sum_{i=1}^{N} z_i(t+1) = \sum_{i=1}^{N} z_i(t) + \sum_{i=1}^{N} \sum_{j \in N_i} w_{ij}\big(z_j(t) - z_i(t)\big). \tag{30}$$

The second summation on the right-hand side of the equation under balanced weights (i.e., $\forall i, j : w_{ij} = w_{ji}$) always equals zero. Now if a link between two nodes i, j fails, the connectivity strength between those two nodes becomes zero (i.e., $w_{ij} = w_{ji} = 0$). Then still $\sum_{i=1}^{N} \sum_{j \in N_i} w_{ij}(z_j(t) - z_i(t)) = 0$ and as a result, $\sum_{i=1}^{N} z_i(t+1) = \sum_{i=1}^{N} z_i(t)$. Thus, the global information (summation of the local information) remains intact. Therefore, if the communications graph remains connected after the failure, the consensus values still converge to the true average (i.e., average of the global information). The proposed algorithm uses consensus networks to access the global information. Thus, it will be robust to any link failures that do not affect the connectivity of the communications networks. Also, when one node fails to communicate with its neighbors, then the rest of the group can continue their operations, provided that their communications graph is connected.

TABLE IV
MONTE CARLO SIMULATION SAMPLING RANGE

	MinValue	MaxValue
$w_i(k)$	0	1
Q_i	20 A.h	30 A.h
$V_i(k)$	210 V	250 V
SoC	0	1
$P_{i,\max}$	0 kW	5 kW

C. Scalability Analysis

In this section, we test the per-node computational scalability of the proposed distributed algorithm. To do so, we perform Monte Carlo simulations. Each node represents a charging station. The range for the number of nodes for the experiments is 10–450. For each value of the number of nodes, we ran 100 Monte Carlo simulations [28].

The parameters in each simulation are randomly sampled from their feasible ranges as shown in Table IV. A random network topology is chosen for each simulation.

The number of operations each node needs to perform until reaching the optimal point $n_{\text{operations}}$ is calculated as follows:

$$n_{\text{operations}} = n_{\text{out}} \times n_{\text{in}} \times \bar{k} \tag{31}$$

where n_{out} and n_{in} are the numbers of outer and inner loops, respectively, of the algorithm prior to convergence and $\bar{k}$ is the average number of neighbors of each node. Basically, $n_{\text{out}} \times n_{\text{in}}$ represents the total number of times the consensus operation is performed at each node, and, according to (22), each consensus operation involves $\bar{k}$ multiplications on an average.

To count the number of outer loops, we count the number of times we have to repeatedly use (21) until all vehicles get a valid allocation of power. To count the number of inner loops, we look at the number of iterations the average consensus needs to reach within 2% of the final value. According to [27], this value can be calculated as

$$n_{\text{in}} = \frac{\ln(0.02)}{\ln(\rho(\boldsymbol{W}))} \tag{32}$$

where $\rho(\boldsymbol{W})$ is the spectral radius of update matrix $\boldsymbol{W}$ in (23).

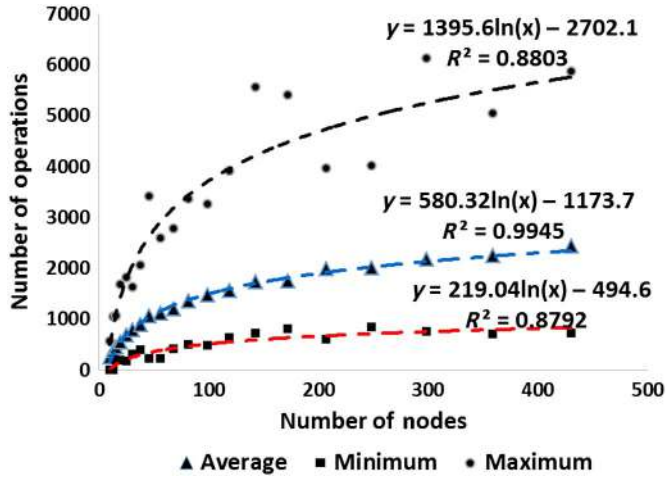

Fig. 8. Computational complexity of CDPDM algorithm as a function of number of nodes (average number of neighbors = 3).

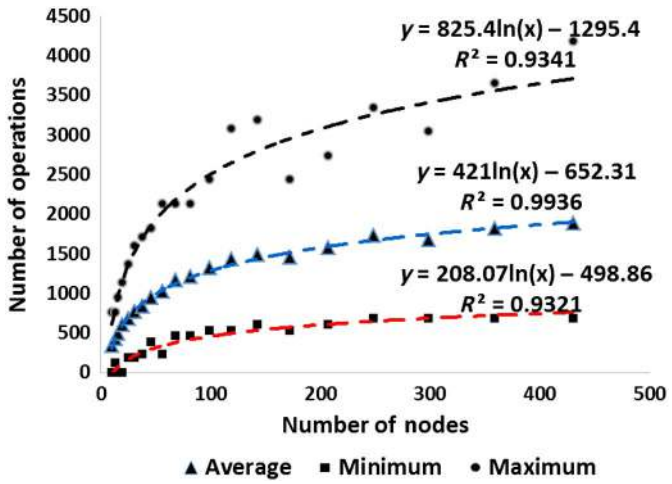

Fig. 9. Computational complexity of CDPDM algorithm as a function of number of nodes (average number of neighbors = 20).

Figs. 8 and 9 show the minimum, maximum, and average number of the operations among 100 random simulations as a function of the number of nodes. The case studies are repeated for $\bar{k} = 3$ and $\bar{k} = 20$. Each dot in the figure corresponds to a set of 100 simulation data.

A logarithmic trend line is fitted to the data points using a least squares error approach. The coefficient of determination (R^2), with a maximum value of 1, represents how well the data is explained by the curve [29]. It can be seen that for both the figures, the logarithmic trend explains the increase in the average computational complexity with $R^2 = 0.99$. In other words, by increasing the number of charging stations, the average computational complexity for the cooperative distributed algorithm grows almost logarithmically rather than exponentially. Therefore, the proposed distributed algorithm is scalable. By noting that each multiplication operation in the algorithm corresponds to a data-packet transfer between two nodes, the per-node communicational burden would exhibit exactly the same scalable behavior.

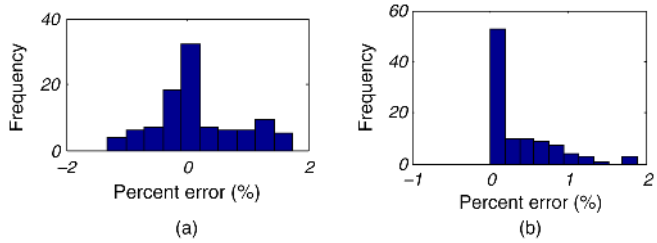

Fig. 10. Distribution of optimization error for CDPDM algorithm with respect to (a) the Interior Point method and (b) SQP.

D. Sub-Optimality of the Algorithm: Benchmarking Against Centralized Algorithms

In this section, we study the sub-optimality of the solutions returned by the proposed distributed algorithm by benchmarking it against two centralized nonlinear optimization algorithms: sequential quadratic programming (SQP) and interior point methods. SQP methods are some of the most successful nonlinear programming algorithms [30] and are used on nonlinear problems where the objective function and the constraints are both continuously differentiable. Interior point methods are also conventional algorithms for solving constrained nonlinear optimization problems [31]. Both of these algorithms are provided by MATLAB through the *fmincon* optimization function.

For both the centralized algorithms, the optimization problem to be solved is the problem represented by (11), prior to the nonlinear approximation of the cost function. To have a fair comparison, the optimality of the solutions for the centralized and distributed algorithms should be measured using the same objective function. Therefore, we use the original objective function of interest in (1) to compare the optimality of the algorithms.

We use Monte Carlo simulations and generate 100 different scenarios where the number of nodes is randomly selected between 10 and 100 and the parameters are randomly sampled from the ranges specified in Table IV. For each simulation scenario, three algorithms are used and the value of the objective function is recorded. Then, the error of the proposed cooperative distributed algorithm with respect to the ith algorithm is calculated as

$$\%e_i = \frac{J_{\text{CDPDM}} - J_i}{|J_i|} \times 100 \tag{33}$$

where J_{CDPDM} is the objective function value using the cooperative distributed algorithm and J_i is the objective function value from the ith algorithm. The distribution of errors is shown in Fig. 10. We can see that the maximum deviation from optimality is 1.8%.

V. Conclusion

In this paper, we introduced a cooperative distributed energy management scheme for community charging of PHEV/PEVs. The main advantages of our approach are preventing the need for a central energy management unit, being more robust against single-link/node failures, and being scalable in terms of single-node computations despite a small amount of sub-optimality ($\sim 2\%$). First, we formulated the charge allocation

as a constrained nonlinear optimization problem and developed a procedure to solve the problem by checking KKT conditions. Then, we decomposed the charge information to local and global parts and proposed a distributed consensus-based algorithm to find the optimal charging policy in each charging time frame using peer-to-peer communications capabilities among charging stations. The performance, scalability, and robustness of the algorithm to single-link/node failures were case-studied.

To apply the proposed algorithm in the real world, practical issues such as EV and charging station communications features, voltage and frequency deviations at the terminals, losses in the power lines, and feeders as well as more complicated battery models should be considered in the distributed optimization process. This will be the future work of the authors.

References

[1] X. Fang, S. Misra, G. Xue, and D. Yang, "Managing smart grid information in the cloud: Opportunities, model, and applications," *IEEE Netw.*, vol. 26, no. 4, pp. 32–38, Jul./Aug. 2012.

[2] J. Bryson and P. Gallagher, "NIST framework and roadmap for smart grid interoperability standards, release 2.0," National Institute of Standards and Technology (NIST), Tech. Rep. NIST Special Publication 1108R2, 2012.

[3] W. Su, H. R. Eichi, W. Zeng, and M.-Y. Chow, "A survey on the electrification of transportation in a smart grid environment," *IEEE Trans. Ind. Informat.*, vol. 8, no. 1, pp. 1–10, Feb. 2012.

[4] J. Wang, C. Liu, D. Ton, Y. Zhou, J. Kim, and A. Vyas, "Impact of plug-in hybrid electric vehicles on power systems with demand response and wind power," *Energy Policy*, vol. 39, no. 7, pp. 4016–4021, Jul. 2011.

[5] K. Clementnyns, E. Haesen, and J. Driesen, "The impact of charging plug-in hybrid electric vehicles on a residential distribution grid," *IEEE Trans. Power Syst.*, vol. 25, no. 1, pp. 371–380, Feb. 2010.

[6] E. Sortomme and M. A. El-Sharkawi, "Optimal charging strategies for unidirectional vehicle-to-grid," *IEEE Trans. Smart Grid*, vol. 2, no. 1, pp. 131–138, Mar. 2011.

[7] C. Liu, K. T. Chau, D. Wu, and S. Gao, "Opportunities and challenges of vehicle-to-home, vehicle-to-vehicle, and vehicle-to-grid technologies," *Proc. IEEE*, vol. 101, no. 11, pp. 2409–2427, Nov. 2013.

[8] T. P. Lyon, M. Michelin, A. Jongejan, and T. Leahy, "Is 'smart charging' policy for electric vehicles worthwhile?" *Energy Policy*, vol. 41, pp. 259–268, Feb. 2012.

[9] F. J. Soares and P. M. Almeida, "Smart charging strategies for electric vehicles: Enhancing grid performance and maximizing the use of variable renewable energy resources," in *Proc. EVS24 Int. Battery Hybrid Fuel Cell Electric Veh. Symp.,* Stavanger, Norway, 2009, pp. 1–11.

[10] S. Bashash, S. J. Moura, J. C. Forman, and H. K. Fathy, "Plug-in hybrid electric vehicle charge pattern optimization for energy cost and battery longevity," *J. Power Sources*, vol. 196, no. 1, pp. 541–549, 2011.

[11] S. Chen, Y. Ji, and L. Tong, "Large scale charging of electric vehicles," in *Proc. IEEE Power Energy Soc. Gen. Meet.,* San Diego, CA, USA, 2012, pp. 1–9.

[12] W. Su and M.-Y. Chow, "Performance evaluation of a PHEV parking station using particle swarm optimization," in *Proc. Power Energy Soc. Gen. Meet.,* Detroit, MI, USA, 2011, pp. 1–6.

[13] C. Jin, J. Tang, and P. Ghosh, "Optimizing electric vehicle charging with energy storage in the electricity market," *IEEE Trans. Smart Grid*, vol. 4, no. 1, pp. 311–320, Mar. 2013.

[14] N. Boucké and T. Holvoet, "Decentralized coordination of plug-in hybrid vehicles for imbalance reduction in a smart grid," in *Proc. 10th Int. Conf. Auton. Agents Multiagent Syst.,* Taipei, Taiwan, 2011, vol. 2, pp. 803–810.

[15] S. Stüdli, E. Crisostomi, R. Middleton, and R. Shorten, "A flexible distributed framework for realising electric and plug-in hybrid vehicle charging policies," *Int. J. Control*, vol. 85, no. 8, pp. 1130–1145, Jun. 2012.

[16] Z. Fan, "A distributed demand response algorithm and its application to PHEV charging in smart grids," *IEEE Trans. Smart Grid*, vol. 3, no. 3, pp. 1280–1290, Sep. 2012.

[17] N. Rotering and M. Illic, "Optimal charge control of plug-in hybrid electric vehicles in deregulated electricity markets," *IEEE Trans. Power Syst.*, vol. 26, no. 3, pp. 1021–1029, Aug. 2011.

[18] H. Rahimi-Eichi and M.-Y. Chow, "Auction-based energy management system of a large-scale PHEV municipal parking deck," in *Proc. IEEE Energy Convers. Congr. Expo.* (ECCE), Raleigh, NC, USA, 2012, pp. 1811–1818.

[19] C.-K. Wen, J.-C. Chen, J.-H. Teng, and P. Ting, "Decentralized plug-in electric vehicle charging selection algorithm in power systems," *IEEE Trans. Smart Grid*, vol. 3, no. 4, pp. 1779–1789, Dec. 2012.

[20] N. Rahbari-Asr and M.-Y. Chow, "Network distributed demand management for optimal large-scale charging of PHEVs/PEVs," in *Proc. IEEE Power Energy Soc. Gen. Meet.,* Vancouver, BC, Canada, 2013, pp. 1–5.

[21] Z. Zhang and M.-Y. Chow, "Convergence analysis of the incremental cost consensus algorithm under different communication network topologies in a smart grid," *IEEE Trans. Power Syst.*, vol. 27, no. 4, pp. 1761–1768, Nov. 2012.

[22] L. Jian, H. Xue, G. Xu, X. Zhu, D. Zhao, and Z. Y. Shao, "Regulated charging of plug-in hybrid electric vehicles for minimizing load variance in household smart microgrid," *IEEE Trans. Ind. Electron.*, vol. 60, no. 8, pp. 3218–3226, Aug. 2013.

[23] A. Mordecai, *Nonlinear Programming: Analysis and Methods.* New York, NY: Dover, 2003.

[24] R. Olfati-saber and R. M. Murray, "Consensus problems in networks of agents with switching topology and time-delays," *IEEE Trans. Automat. Control*, vol. 49, no. 9, pp. 1520–1533, Sep. 2004.

[25] W. Zeng, M.-Y. Chow, and P. Ning, "Secure distributed control in unreliable D-NCS," in *Proc. IEEE Int. Symp. Ind. Electr.* (ISIE). Hangzhou, China, 2012, pp. 1858–1863.

[26] K. Morrow, D. Karner, and J. Francfort, "Plug-in hybrid electric vehicle charging infrastructure review," *US Department of Energy-Vehicle Technologies Program,* 2008.

[27] L. Xiao and S. Boyd, "Fast linear iterations for distributed averaging," *Syst. Control Lett.*, vol. 53, no. 1, pp. 65–78, Sep. 2004.

[28] M. H. Kalos and P. A. Whitlock, *Monte Carlo Methods.* Hoboken, NJ: Wiley, 2008.

[29] H. J. Motulsky and L. A. Ransnas, "Fitting curves to data using nonlinear regression: A practical and nonmathematical review," *FASEB J.*, vol. 1, no. 5, pp. 365–374, 1987.

[30] P. T. Boggs and J. W. Tolle, "Sequential quadratic programming," *Acta Numer.*, vol. 4, no. 1, pp. 1–51, 1995.

[31] M. H. Wright, "The interior-point revolution in optimization: History, recent developments, and lasting consequences," *Bull. Amer. Math. Soc.*, vol. 42, no. 1, pp. 39–57, Sep. 2004.

Navid Rahbari-Asr (S'11) received the B.S. degree in electrical engineering from the University of Tabriz, Tabriz, Iran, in 2008. In 2011, he received the M.Sc. degree in control engineering from Tarbiat Modares University, Tehran, Iran. He is currently working toward the Ph.D. degree with the Advanced Diagnosis Automation and Control Laboratory, North Carolina State University, Raleigh, NC, USA.

His research interests include distributed control, distributed optimization, big data, and computational intelligence with applications to smart grids.

Mo-Yuen Chow (S'81–M'82–SM'93–F'07) received the B.S. degree in electrical and computer engineering from the University of Wisconsin–Madison, Madison, WI, USA, in 1982, and the M.Eng. and Ph.D. degrees in electrical engineering from Cornell University, Ithaca, NY, USA, in 1983 and 1987, respectively.

He worked as an Assistant Professor and Associate Professor with the Department of Electrical and Computer Engineering, North Carolina State University, Raleigh, NC, USA, in 1987 and 1993, respectively, where he has been a Professor since 1999. He is also a Changjiang Scholar and a Visiting Professor with Zhejiang University, Zhejiang, China. He has established the Advanced Diagnosis and Control Laboratory at North Carolina State University. He has published one book, several book chapters, and more than 200 journals and conference articles. His recent research focuses on distributed control, big data, and fault management on smart grids, batteries, and robotic systems.

He is a Co-Editor-in-Chief of IEEE Transactions on Industrial Informatics and Editor-in-Chief of IEEE Transactions on Industrial Electronics 2010–2012. He has received the IEEE Region-3 Joseph M. Biedenbach Outstanding Engineering Educator Award, the IEEE Eastern North Carolina Section (ENCS) Outstanding Engineering Educator Award, the IEEE ENCS Service Award, and the IEEE Industrial Electronics Society (IES) Anthony J. Hornfeck Service Award. He is also a Distinguished Lecturer for the IEEE IES.